

Chapter 8

Turbulent Transport Phenomena: Qualitative Analysis

8.1 Generic turbulent flows and convective processes

Most practical problems of fluid flow and transport processes involve complex geometries and boundary conditions so that solutions can be obtained only by a numerical method, using powerful computers, Fig. 8.1. However, for studying physics of transport phenomena, for deriving mathematical models and for validating models and computational codes, it is instructive to consider some simple cases where certain phenomena can be regarded as dominant whereas others can be neglected. Mathematically this means that some terms in the governing equations can be omitted. These flows possess some similarity features which enable scaling with only a few reference parameters. Major properties of such flows can often be evaluated using simple tools such as similarity and dimensional arguments. Governing equations can be simplified to the level where the solutions can be obtained analytically or using simple computational methods, (e.g. partial differential equations can be reduced to ordinary ones, or elliptic partial differential equations can be reduced to a parabolic form, etc.). Because of their characteristic features which are pertinent to the whole class, such flows are also called *generic*, *canonical* or *reference* flow classes. In many complex situations a reasonable insight into the problem can be gained by decomposing the flow domain into zones which correspond to some of the generic flow classes, Fig. (8.2). Such an *a priori* analysis is also useful before deciding on the appropriate level of mathematical model and computational code to be applied for obtaining the solution.

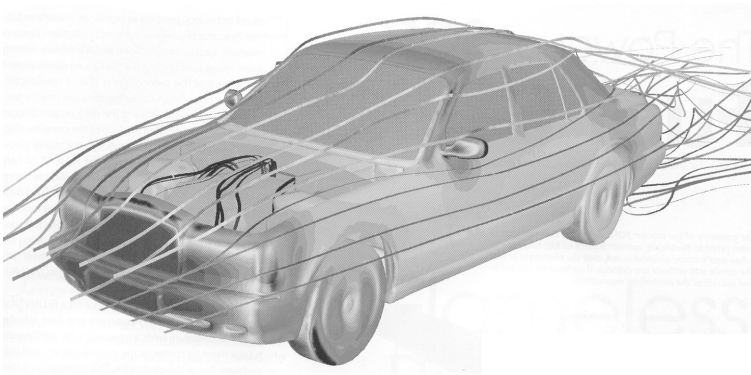


Figure 8.1 Computer simulation of flow around an automobile (FLUENT News, 2002).

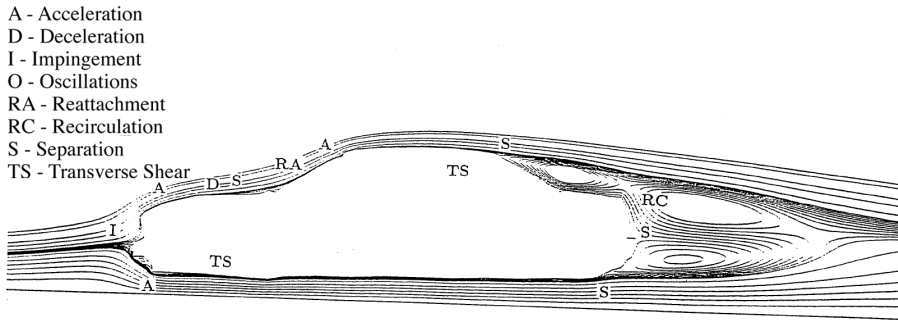


Figure 8.2 Identification of dominant flow phenomena in flow around an automobile.

The following basic generic flows can be identified:

- Homogeneous turbulent flows
- Thin shear flows (parabolic, boundary-layer flows):
 - *free* thin shear flows (single plane and round jets, mixing layers, far-wakes behind bluff bodies)
 - *wall* boundary layers
- Impinging (stagnation) flow regions
- Separating flow regions
- Recirculations
- Swirling flows
- Flows with system rotation
- Flows dominated by thermal and/or concentration buoyancy
- ...

In addition to the above classification, we can also distinguish internal from external flows: the first category denotes the flows fully bounded by walls (e.g. flow in pipes and conduits, in engine cylinders, heat exchangers, chemical reactors, furnaces, etc.), whereas the second category denotes flows around bodies (e.g. vehicles - cars, ships, airplanes, rockets - or a part of a vehicle, e.g. wing, windmill or helicopter blades, etc.).

Although this classification is based solely on the feature of the velocity field and momentum equation, we may in all cases mentioned encounter heat and mass transfer. If the flow is driven by the imposed pressure gradient (pump or compressor) the thermal and concentration fields can be treated as *passive scalars*, meaning that they do not affect the velocity field and its turbulent fluctuations. Such transport processes are known as *forced convection*. If the flow is driven, or influenced by density difference, caused either by a

strong temperature or concentration gradient, or both, we are talking about *active* fields. A separate class of flows are those driven only by thermal or concentration buoyancy (natural convection). If both the forced and natural convection are present, we talk about *mixed convection*, (e.g in space heating, cooling and air-conditioning).

8.1.1 Homogeneous turbulent flows

Homogeneous flows are characterised by homogeneity (invariance to coordinate system translation) at least in one coordinate direction. Some typical examples are shown in Fig. 8.3. Homogeneous flows appear rarely in practice and even more rarely in na-

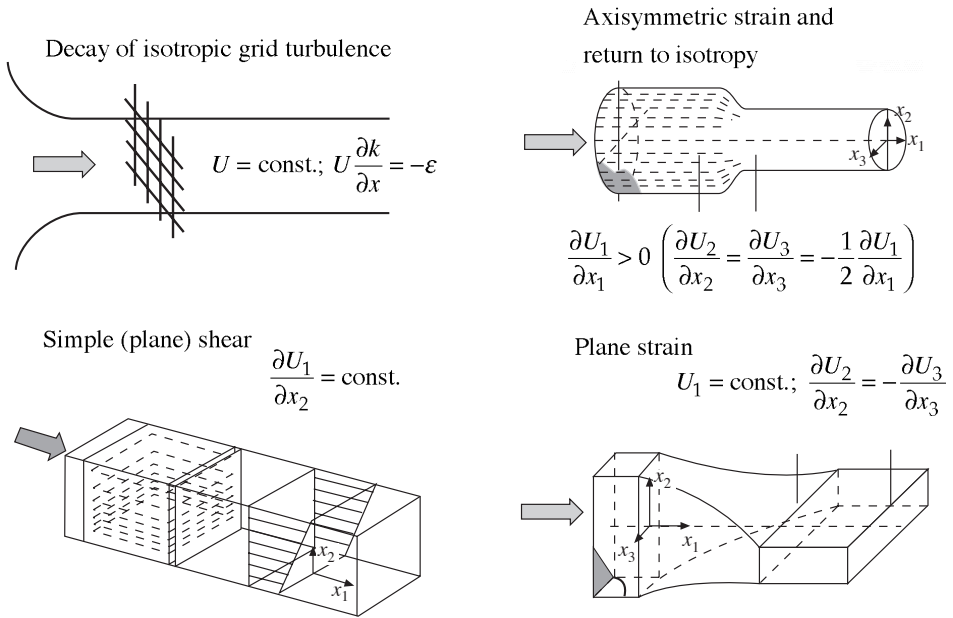


Figure 8.3 Some generic homogeneous flows (note that in all cases, the coordinate x_1 denotes the streamwise direction).

ture, but nevertheless they are very instructive for studying turbulence physics, especially the response of initially isotropic turbulence in a uniform flow when subjected to a specific simple deformation, usually just one component of the rate of strain $S_{ij} = 0.5(\partial U_i/\partial x_j + \partial U_j/\partial x_i)$. For some homogeneous flows we can even get analytical solutions of the Reynolds-averaged equations. Homogeneous flows are also essential test flows for turbulence models or any approximate theories of turbulence, and have served for determining - assigning the values, or for verifying empirical coefficients that are unavoidable in turbulence modelling.

The simplest case shown is the decay of isotropic turbulence ($\bar{u}_1 = \bar{u}_2 = \bar{u}_3 = \sqrt{2/3k}$ and $\overline{u_i u_j} = 0$ if $i \neq j$). Such a turbulence is usually generated in laboratory wind tunnels by a grid made of round, square or other bars (see also Fig. 7.14). Although initially inhomogeneous and anisotropic (the latter reflecting the geometry of the grid), intensive

mixing, vortex stretching and energy cascading will make the turbulence fully isotropic at a sufficient distance downstream. Because there is no flow deformation ($S_{ij} = 0$), no body force or any other source of turbulence downstream, velocity fluctuations will gradually weaken and disappear. Turbulence kinetic energy will decay and eventually dissipate into heat. The decay law, established experimentally, is used to determine one of the coefficients in turbulence models, as discussed in the next chapter.

In the next example, isotropic turbulence in a uniform flow is subjected to axisymmetric strain $S_{11} = \partial U_1 / \partial x_1 > 0$ by passing through an axisymmetric contraction. It follows from the continuity equation that the other two components of the normal straining are both negative and equal to half of the imposed strain rate, i.e. $S_{22} = S_{33} = -0.5S_{11}$. Note that shear straining is zero everywhere, $S_{ij} = 0$ if $i \neq j$. This deformation generates anisotropic turbulence characterised by normal stress inequality, i.e. $\overline{u_2^2} = \overline{u_3^2} > \overline{u_1^2}$. In the rest of the duct in the absence of any other source of turbulence (effects of walls are here neglected because they are confined to thin wall boundary layers), the turbulence will return to the isotropic state, while continuously decaying.

The plane strain has similar qualitative effects on turbulence, but affecting different stress components as determined by the active strain-rate components. In Fig. 8.3 the plane-strain flow is a specific case in which the streamwise velocity U_1 remains constant and the continuity equation imposes a specific relationship between the two active normal-strain component, i.e. $S_{22} = -S_{33}$.

The last case is a simple plane (homogeneous) shear, which can be generated in laboratory circumstances by placing parallel solid sheets of different length, spacing or different roughness, selected in such a way that they would generate a linear velocity profile across the wind tunnel cross-section. Thus, the only active straining is the plane shear $S_{12} = 0.5\partial U_1 / \partial x_2$.

8.1.2 Thin shear flows

Thin shear flows are very common either on their own or they appear in some regions of a complex flow. As the tells us, they are characterised by a strong though thin shear layer which evolves (grows or shrinks) gradually in the main flow direction Their main feature is the parabolic character of the averaged equations, which follows after applying Prandtl boundary layer approximations:

$$\delta \ll L; \quad U_1 \gg U_2 \quad \text{and} \quad \frac{\partial U_1}{\partial x_2} \gg \frac{\partial U_1}{\partial x_1} \quad (8.1)$$

where "1" denotes the streamwise (main flow) direction and x_2 the normal direction, δ is the shear layer thickness and L denotes the characteristic streamwise direction (length of the layer considered). The parabolic character of the equations emerges after neglecting all second mean-velocity derivatives except in the normal direction, i.e. $\partial^2 U_1 / \partial x_2^2 \gg \partial^2 U_1 / \partial x_1^2$. Thin shear flows can further be divided into thin *free* shear flows (jets, mixing layers, wakes behind bluff bodies sufficiently far downstream, beyond the recirculation zone) and thin *wall* shear layers (wall boundary layers, wall jets, flows in circular pipes and plane channels). Most wall boundary layers can be treated as two-dimensional (in

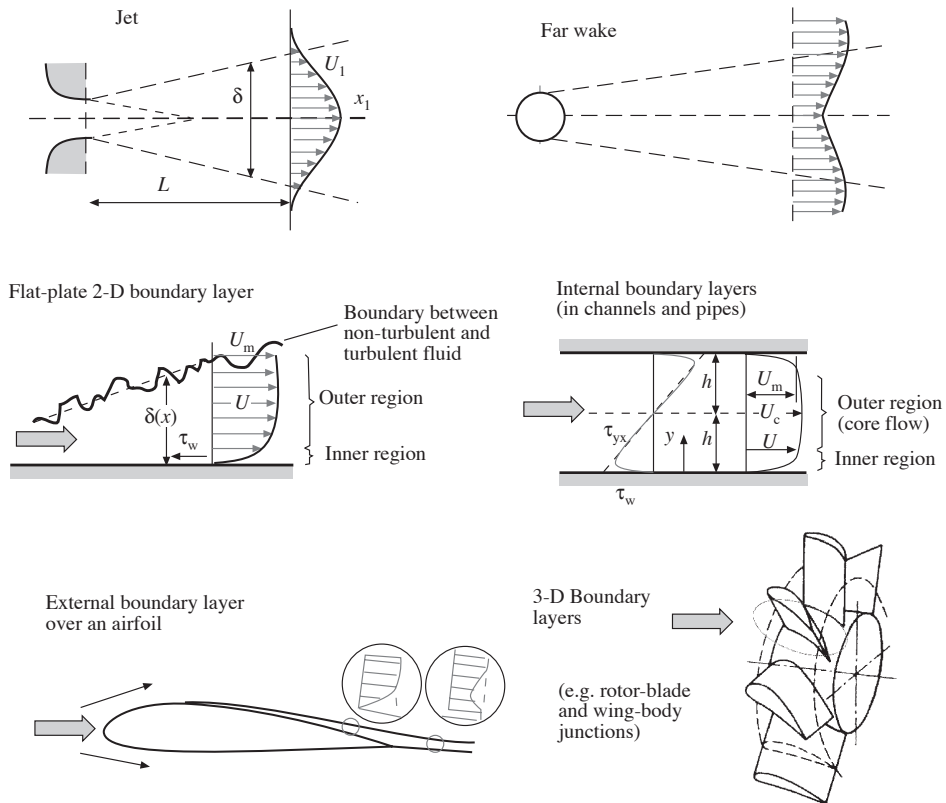


Figure 8.4 Some generic thin free and wall shear flows.

the mean) because their thickness is also much smaller than the spanwise variations, if any. Three-dimensional boundary layers develop along corners, i.e. at aircraft wing-body junctions, or at blade-rotor junctions in turbomachinery. The equations still retain a parabolic character but with parabolicity applied to two lateral dimensions - two thin wall shear layers on the two connecting walls. Some examples of thin shear flows are shown in Fig. 8.4.

8.1.3 More complex "generic" flows

A number of other, relatively simple flows are also known as generic because each is characterised by a specific feature that dominates the flow and turbulence dynamics. Such flows have been extensively studied analytically, experimentally and computationally in order to gain better insight into turbulence physics, but also to provide data for calibration and validation of turbulence models and other approximate theories. Fig. 8.5 shows several "more" complex generic flows.

The first example is the flow behind a backward-facing step ("back-step flow"), which has long served as a paradigm of separating flows. It is characterised by flow separation at the step edge (fixed point/line separation), followed by a recirculation bubble and shear

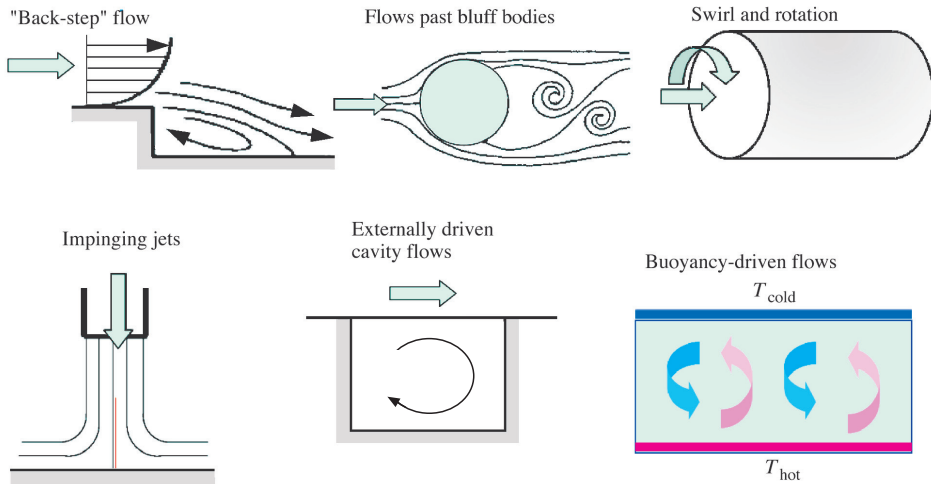


Figure 8.5 Some more complex generic flows.

layer reattachment. Flows past simple bluff bodies with curved contours (such as cylinders or spheres) have also served to study flow separation and wakes. Here the position of the separation is not fixed, but moves in time over the smooth body surface in an oscillating manner causing a periodic vortex shedding behind the body. Swirl and system rotation, common in turbomachineries, combustion devices, cyclone separators and in natural flows, impose also specific effects on turbulence dynamics. Swirls have been studied in simple generic swirling jets or swirls confined in a short or long pipe. Likewise, rotational effects have been analyzed in simple flows such as plane channels or pipes subjected to rotation around one of the coordinate axes. Impinging jets, in addition to being of practical relevance (used widely to enhance cooling, heating or drying), are also of canonical interest because one can study turbulence dynamics in the stagnation region, in the curved shear layer at the jet edge and in the wall jet (plane or radial) away from the jet centre. Fluid movement and turbulence dynamics in a complete enclosure (a cavity), driven by a moving wall on one of the cavity sides, is also of generic interest because here the flow is independent from the external conditions and fully controlled by the imposed wall movement. Another generic class are the flows driven purely by thermal (or concentration) buoyancy that are of interest in many technological applications, but also for studying the movement of air in the Earth's atmosphere, of water in lakes and oceans, or of magma in the Earth's interior. Turbulence dynamics in a fluid layer trapped between the two walls of unequal temperature, of which the bottom wall is warmer than the top wall, known as Rayleigh-Bénard convection, has long served as a paradigm of thermal convection. Geometrically very simple, it can be easily reproduced in a laboratory or by computer simulations, and yet it possesses most of the features of real-scale buoyancy-driven turbulent flows.

Generally a turbulence model can be regarded as sufficiently reliable and thus appli-

cable for predicting unknown complex situations if it can reproduce experimental or other (e.g. DNS, LES) results in most if not all of the generic flow cases.

Of the listed generic flows, in more detail we consider only the wall boundary layers, because of their importance and relevance for turbulence modelling.

8.2 Turbulent wall boundary layer

Wall boundary layers represent one of the most important classes of flows, because many flows of practical relevance are bounded in part or as a whole by solid walls. The significance of boundary layers is especially relevant to deriving approximate methods for treating wall boundary conditions, which are essential in predicting accurately wall-bounded flows, heat and mass transfer. The simplest form is a boundary layer over a flat plate at zero pressure gradient, which can be analyzed using simple similarity arguments. At high Reynolds numbers, after a short transition length, initially laminar flow becomes fully turbulent and independent of fluid viscosity, Fig. (8.6). However, a solid wall suppresses the velocity and its fluctuation ('no-slip conditions'), so that, irrespective of the Reynolds number, there is always a thin *viscous sublayer* attached to the wall. Between the viscous sublayer and the fully turbulent layer there is a transitional 'buffer' zone where both the viscous and inertial forces are of importance.

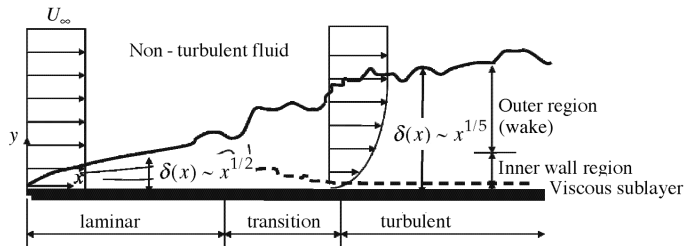


Figure 8.6 Scheme of a wall boundary layer developing along a flat plate.

8.2.1 Similarity analysis and velocity distribution

We consider a constant-pressure boundary layer on a flat plate and apply similarity and dimensional analysis. It is well known that in a laminar boundary layer the velocity, temperature and concentration profiles possess a self-similarity, that is, when scaled (non-dimensionalised) with characteristic velocity and length scales, they exhibit the same form, irrespective of the position along the flow. We can expect that the same similarity features are preserved in turbulent boundary layers, i.e.

$$\frac{U}{\mathcal{U}} = f\left(\frac{y}{\mathcal{L}}\right) \quad (8.2)$$

where \mathcal{U} and \mathcal{L} are the characteristic velocity and length scales, respectively, and f is a general function (all to be determined). We can now list all parameters that are expected to influence the velocity field. For the so-called *inner wall region*, where the flow and

turbulence are dominated solely by the wall, the list must include the wall shear stress τ_w (friction), the local flow properties (density ρ and viscosity μ) and the local wall distance y , i.e.

$$U = f(\tau_w, \rho, \mu, y, \dots) \quad (8.3)$$

(where stands for other parameters not accounted for here, e.g. wall roughness characteristics if the wall is not smooth, pressure gradient if it is very different from zero, mass blowing or suction through the wall if the wall is not impermeable, fluid temperature if the thermal field is active, etc.).

Dimensional analysis yields the following nondimensional expression:

$$\frac{\rho U^2}{\tau_w} = f\left(\frac{y^2 \rho \tau_w}{\mu^2}\right) = f\left(\frac{y^2 \tau_w}{\nu^2 \rho}\right) \quad (8.4)$$

By comparing the above two equations it follows that the characteristic velocity is

$$u = \sqrt{\frac{\tau_w}{\rho}} = U_\tau \quad (8.5)$$

U_τ is called the *friction velocity*. The characteristic length, known also as the *viscous length* can now be determined as

$$\mathcal{L} = \nu \sqrt{\frac{\rho}{\tau_w}} = \frac{\nu}{U_\tau} \quad (8.6)$$

U_τ and ν/U_τ are known as the *inner wall scales* for turbulent wall boundary layers and the general nondimensional similarity expression can be written as

$$\frac{U}{U_\tau} = \left(\frac{y U_\tau}{\nu}\right), \quad \text{or} \quad U^+ = f(y^+) \quad (8.7)$$

It still remains now to determine the function ' f '! However, because of a multi-layer structure of even the relatively thin inner part of a turbulent wall boundary layer, we need to separately treat the viscous and fully turbulent zone. The major difference between these two zones is that in the viscous sublayer the viscous force (represented by μ) is dominant over the inertial force, hence the parameters related to mass (or fluid density) must disappear from the expression for the non-dimensional velocity. In the fully turbulent zone it is the other way round: viscosity should not appear in the expression. In other words, in the viscous sublayer, the viscous stress $\tau = \mu(dU/dy)$ is dominant, whereas in the turbulent zone it is negligible as compared with the turbulent shear stress $\tau^t = -\rho \bar{u}v$. A mechanical analogy with two springs (a spiral and a plate spring) of different stiffness, connected with a flexible joint, illustrates in which way the molecular viscosity (here corresponding to the stiffness C_1 of the spiral spring) affects the velocity profile in the turbulent region (here represented by the deformed shape of the plate spring), Fig. 8.7. The deformation of the plate spring is fully determined by its stiffness C_2 which corresponds to the intensity of turbulent mixing that can be represented by "turbulent" viscosity (see next Chapter).

Under the same force the plate spring will always have the same deformed shape, but its position will depend on the stiffness of the spiral spring. Likewise, we can expect that the velocity profile in the turbulent zone will always have the same profile for the given turbulent viscosity, but the velocity magnitude will depend on the molecular viscosity.

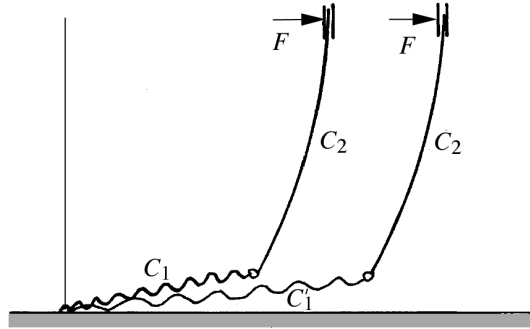


Figure 8.7 Mechanical analogy of a wall boundary layer: the spring stiffness corresponds to fluid effective (molecular or turbulent) viscosity.

Viscous sublayer. The only form of the function f in Eq. (8.7), which ensures that U is independent of density ρ is $f = 1$. This gives the velocity distribution law in the viscous sublayer as

$$U^+ = y^+ \quad (8.8)$$

which means that the mean velocity varies linearly with the distance from the wall. Note that equation (8.3) is now reduced to $U = f(\tau_w, \mu, y)$ and no ρ appears.

Turbulent wall zone. Here we expect that the shape of the velocity profile will be independent of viscosity. The profile shape can be characterised by the velocity gradient, thus we can express this condition by postulating that

$$\frac{dU}{dy} \neq f(\mu) \quad (8.9)$$

and, since $U = U_\tau f(y^+)$,

$$\frac{dU}{dy} = U_\tau \frac{df}{dy^+} \cdot \frac{dy^+}{dy} = \frac{U_\tau^2}{\nu} \frac{df}{dy^+} \quad (8.10)$$

df/dy^+ must be proportional to ν and non-dimensional. The only form which satisfies these conditions is

$$\frac{df}{dy^+} \propto \left(\frac{yU_\tau}{\nu} \right)^{-1} \quad (8.11)$$

or,

$$\frac{df}{dy^+} = \left(\kappa \frac{y U_\tau}{\nu} \right)^{-1} = \frac{1}{\kappa y^+} \quad (8.12)$$

where κ is a proportionality constant (known as Von Kármán constant, $\approx 0.4 - 0.42$). Hence,

$$\frac{dU}{dy} = \frac{U_\tau^2}{\nu} \frac{1}{\kappa y^+} \quad (8.13)$$

or in nondimensional form

$$\frac{dU^+}{dy^+} = \frac{1}{\kappa y^+} \quad \text{or} \quad dU^+ = \frac{1}{\kappa y^+} dy^+ \quad (8.14)$$

Note that now $dU/dy = f(\tau_w, \rho, y)$ and no μ appears.

After integration the result is

$$U^+ = \frac{1}{\kappa} \ln y^+ + B = \frac{1}{\kappa} \ln(E y^+) \quad (8.15)$$

where $E \approx 9.5$ and $B \approx 5.5$ are the integration constants (note $B = \frac{1}{\kappa} \ln E$), determined experimentally and more recently confirmed by DNS. This expression is known as the *universal logarithmic law* and has been verified by numerous experiments both in wall boundary layers and in the near wall region in plane channel and pipe flows.

Outer wall zone. In the outer region of a wall boundary layer, as well as in the core region of a plane channel or a pipe flow, the effect of the wall is minor and the friction velocity U_τ can not be used as a scaling parameter. Instead, the free stream velocity U_∞ and in the channel and pipe flows the maximum velocity are used as the characteristic velocity scales, whereas the boundary layer thickness δ and the pipe radius (channel half-width) are the characteristic length scales. Here a power law

$$\frac{U}{U_\infty} = \left(\frac{y}{\delta} \right)^n \quad (8.16)$$

is found to fit the experimental data, with $n = 1/7$ to $1/10$ (smaller exponent corresponds to higher Reynolds numbers)

A plot of velocity profiles in linear and semi-logarithmic coordinate systems, with different zones is presented in Fig. 8.8

8.2.2 Temperature distribution

The same similarity and dimensional arguments can be applied to derive the universal distribution of passive scalars, e.g. the mean temperature. Because the wall temperature T_w is not zero, we will express the relative temperature $(T - T_w)$ in terms of possible dependent variables (see the energy equation):

$$(T - T_w) = f_T(\tau_w, \rho, \mu, y, c_p, q_w, \lambda, \dots) \quad (8.17)$$

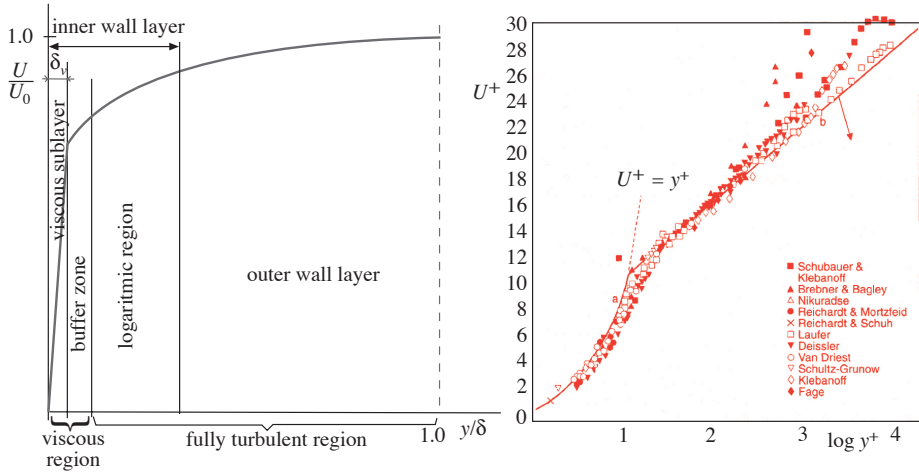


Figure 8.8 Velocity profile and characteristic regions in a wall boundary layer. Right: a collection of experimental results plotted in semi-logarithmic coordinates (Monin & Yaglom, 1973).

Dimensional analysis leads to the non-dimensional form

$$\frac{\rho c_p (T - T_w) \sqrt{\tau_w / \rho}}{\dot{q}_w} = f_T \left(\frac{y \sqrt{\tau_w / \rho}}{\nu}, \frac{c_p \rho \nu}{\lambda} \right) \quad \text{or} \quad T^+ = f_T(y^+, \text{Pr}) \quad (8.18)$$

where c_p is the specific heat, λ is the heat conductivity of the fluid, \dot{q}_w is the wall heat flux, and Pr is the molecular Prandtl number. Note the analogy between the wall fluxes of heat \dot{q}_w and momentum τ_w , and of the corresponding diffusivities, $\alpha = \lambda / (\rho c_p)$ and ν . Following the same argument as for the velocity field we can derive the expressions for the universal distribution of the mean temperature:

Molecular (conductive) sublayer:

$$T^+ = \text{Pr} y^+ \quad (8.19)$$

Wall turbulent zone (the logarithmic layer):

$$T^+ = \frac{1}{\kappa_T} \ln y^+ + B_T(\text{Pr}) \quad (8.20)$$

where κ_T is the Von Karman constant for the temperature field (≈ 0.38)

It should be noted that for fluids with $\text{Pr} = \mathcal{O}(1)$ (for air and most common gases at room temperature $\text{Pr} \approx 0.7$ and for water $\text{Pr} = 7 - 13$) the velocity and temperature boundary layers are very similar (similar thicknesses, similar distributions of mean velocity, temperature and *rms* of turbulent fluctuations, Fig. 8.9). However, for fluids with very

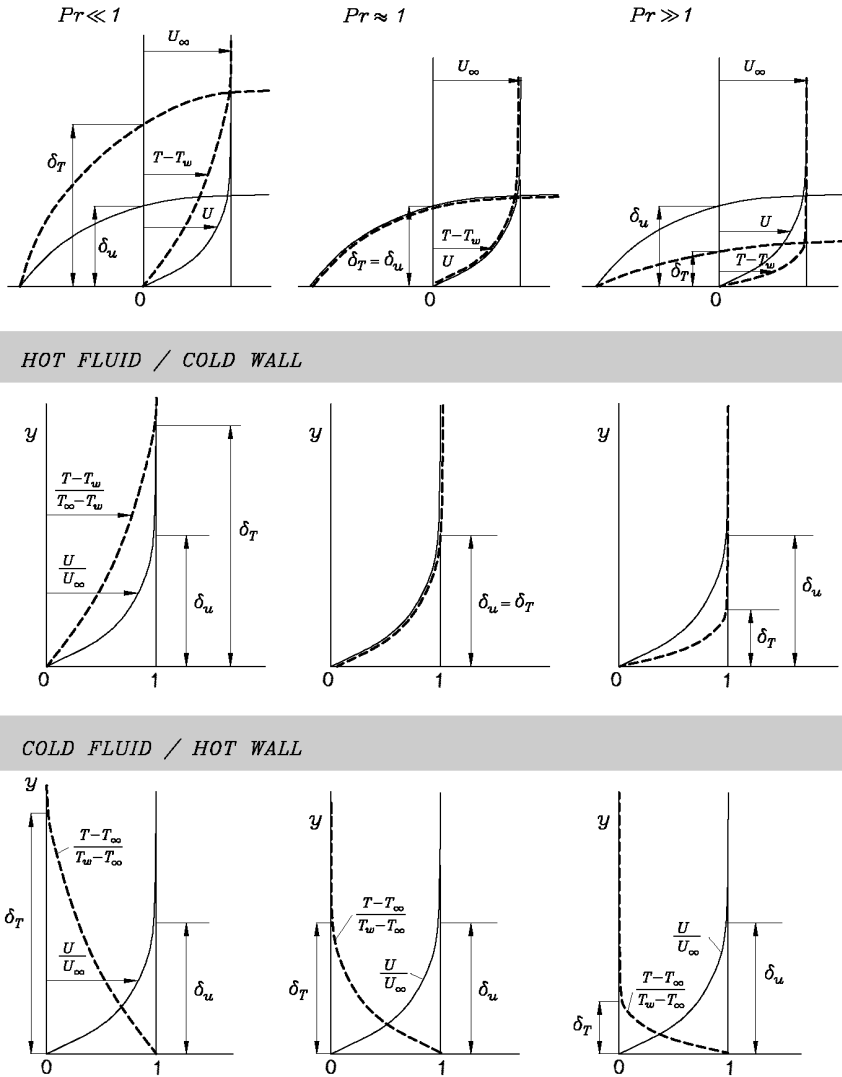


Figure 8.9 Velocity and temperature distribution across a wall boundary layer for fluids with different Prandtl numbers.

low Pr numbers (e.g. liquid metals, for mercury $Pr \approx 0.015$, for liquid sodium $Pr = 0.002$) the conductive sublayer is much thicker than the viscous sublayer and irrespective of turbulence intensity, heat is transported primarily by conduction. In contrast, for high Pr fluids (e.g. for engine oil $Pr = \mathcal{O}(10^3 - 10^4)$), the conductive layer is very thin, acting as an insulator. The effect of Pr number on the logarithmic temperature distribution is accounted for by free constant $B_T(Pr)$ in expression 8.20, which takes different values for different fluids. For $Pr = \mathcal{O}(1)$, $B_T \approx 4.6$. For highly conducting fluids with $Pr \ll 1$, $B_T \approx 1.5$ and for poorly conducting fluids with $Pr \gg 1$, $B_T = 15Pr^{2/3}$.